IJARSCT
International Journal of Advanced Research in Science, Communication and Technology
International Open-Access, Double-Blind, Peer-Reviewed, Refereed, Multidisciplinary Online Journal
ISSN: 2581-9429
Volume 6, Issue 8, April 2026
Impact Factor: 8.2

Transition-Metal Diselenophosphinate Complexes as Single-Source Precursors for "2D Nanomaterial Thin Films and Energy Applications"

Digvijay Chougule and Chitra Gurnani
Department of Chemistry
Ecole Centrale School of Engineering, Mahindra University, Hyderabad, Telangana, India

Abstract: *Two-dimensional (2D) metal chalcogenide nanomaterials have attracted growing interest due to their atomic-scale thickness, high surface-to-volume ratio, and layer-dependent electronic properties, making them promising candidates for advanced energy conversion and storage technologies. Among emerging synthetic approaches, the transition-metal diselenophosphinate complexes have gained attention as efficient single-source molecular precursors for the controlled fabrication of 2D metal selenide thin films. These precursors offer well-defined metal–selenium stoichiometry, tunable coordination environments, and favorable thermal decomposition behavior, enabling low-temperature and solution-processable routes to phase-pure thin films. The various deposition techniques including solvothermal synthesis, hot injection method, and chemical vapor deposition are evaluated with respect to film uniformity, scalability, and structural control. 2D metal selenide thin films are correlated with their functional performance in energy-related applications, such as photovoltaics, rechargeable batteries, super capacitors, and electro catalysis.*

Keywords: Transition metal diselenophosphinates, Single source precursors, Transition metal selenides (TMS), 2D nanomaterials, thin film deposition techniques, Energy applications

1. Introduction

The scale of the current global energy crisis demands the proposal of novel, inventive and practical solutions. A growing global population, accelerating globalization and, an expansive economy reliant on fossil fuel reserves has led to a rise in energy demand, as depicted in Figure 1.1. This rise has placed the natural, already depleting resources of the world under increasing pressure. The finite and polluting nature of these resources has led to the need for clean, renewable technologies to be developed. Technologies capable of satisfying the global energy demands through sustainable means would ease the reliance on fossil fuels and reduce the irrevocable environmental damage caused[1]

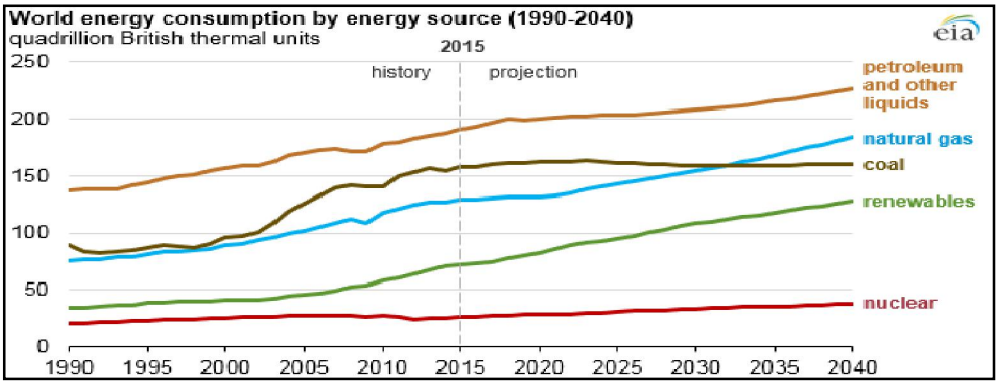

Fig-1.0 Worldwide energy consumption by energy source.[1]

DOI: 10.48175/IJARSCT-33123

IJARSCT
International Journal of Advanced Research in Science, Communication and Technology
International Open-Access, Double-Blind, Peer-Reviewed, Refereed, Multidisciplinary Online Journal
ISSN: 2581-9429
Volume 6, Issue 8, April 2026
Impact Factor: 8.2

To overcome this issues the researcher focused on the coordination chemistry of chalcogenides based metal complexes have a long history, [2–4] and their use as single source precursors (SSP) for materials synthesis, thin films, alloys, and/or polymer composites is widely reported [5,6]. However, in contrast to sulfur based SSPs, the work on molecular precursors containing the higher congeners, have only progressed in the last two decades. The lack of the driving force, in the advancement of the Se and/ or Te based precursors, was the comparatively limited knowledge of the practical applications of the heavier metal chalcogenides. Similarly, the tedious and sometimes complex synthetic methodologies, pose another hurdle in the synthesis and understanding of their chemistry. Nonetheless, developments in the synthetic routes and their usage in industrial applications, especially as low band gap materials for IR and photovoltaic devices, has resulted in the rapid growth of these materials recently.

Nanomaterials have been widely investigated for applications across diverse technological domains, owing to their enhanced physical and chemical properties compared to their bulk analogues. These properties are highly sensitive to microstructural parameters, including chemical composition (stoichiometry), atomic arrangement, crystallinity, and particle dimensions. Even minor deviations in the elemental composition of binary or ternary nanostructures can lead to substantial changes in their functional behavior. Consequently, the development of well-controlled and reliable synthetic strategies is essential to achieve reproducible nanomaterials with precisely tailored size, morphology, and composition and Significant advancements have been achieved in the synthesis of nanostructures and thin films through various chemical routes. Nevertheless, conventional dual- or multi-precursor approaches often suffer from intrinsic limitations related to compositional control. Variations in precursor reactivity, vapour pressure, or decomposition kinetics can result in batch-to-batch inconsistency and undesired stoichiometric deviations in the final product. In contrast, single-source precursors (SSPs) offer notable advantages by incorporating preformed metal–chalcogen bonds within a single molecular entity. This intrinsic bonding facilitates the formation of materials with improved compositional uniformity, reduced defect density, and enhanced phase purity. The single-source precursors are versatile and can be utilized for both nanoparticle synthesis and thin-film fabrication. However, the rational design of effective SSPs requires careful consideration of several critical parameters. High chemical purity is essential, as trace impurities may induce stoichiometric imbalance or promote the formation of unwanted secondary phases. The synthesis of SSPs should ideally involve straightforward, low-step procedures and employ reagents with minimal environmental and health hazards wherever possible. Additionally, the precursors should exhibit sufficient thermal and chemical stability to allow long-term storage and facile characterization. From a practical perspective, SSPs must be amenable to scale-up without excessive complexity, and both the precursors and synthetic processes should be economically viable. For thin-film deposition via solvothermal synthesis, chemical bath deposition, spin coating, and low-pressure chemical vapor deposition (LP-CVD), adequate volatility below the decomposition temperature is a crucial requirement. In aerosol-assisted chemical vapor deposition (AA-CVD), although volatility constraints are relaxed, good solubility in compatible solvents is necessary to ensure uniform aerosol generation and film growth. Furthermore, clean thermal decomposition at the substrate surface is essential, with volatile by-products that can be efficiently removed. Lower precursor decomposition temperatures are particularly desirable, as they contribute to energy-efficient and environmentally deposition processes.

Diselenophosphinates are well known ligands and their early synthesis dated back to 1960s [7]. The previous reported protocols for preparation of diselenophosphinates salts were tedious involving difficult reaction conditions. Diselenophosphinates constitute an important class of ligands for coordination complexes and have attracted attention as efficient extractant for heavy, rare-earth, and Trans uranium elements. In addition, these compounds have emerged as promising candidates in energy applications and serve as versatile precursors in organic and organoelemental synthesis[8]. However, synthetic methods have developed over time. The different strategies, a facile and robust method is to prepare alkali metal salts of diselenophosphinates [9]. The one-pot synthesis is highly efficient and excellent yields can be obtained within a short time. This review presents the first comprehensive consolidation of the chemistry of diselenophosphinates. It offers a systematic overview of established synthetic methodologies while also highlighting recent progress in their functional applications.

IJARSCT
International Journal of Advanced Research in Science, Communication and Technology
International Open-Access, Double-Blind, Peer-Reviewed, Refereed, Multidisciplinary Online Journal
ISSN: 2581-9429
Volume 6, Issue 8, April 2026
Impact Factor: 8.2

Conventional method-

The earliest and most widely adopted routes for the preparation of diselenophosphinates rely on reactions between selenophosphinic chlorides, $R_2P(Se)Cl$, or monochlorophosphines, R_2PCl, and selenium-based nucleophiles such as sodium selenide (Na_2Se) or sodium hydroselenide (NaHSe). These synthetic approaches were primarily established during the mid-to-late twentieth century. Despite their historical importance, these methodologies suffer from inherent constraints, as they predominantly yield diselenophosphinates in the form of sodium salts, thereby limiting their synthetic versatility. After that sodium salt reacts with metal chloride to give a such a types of metal complex see in below fig 2.0 The conventional routes to alkali metal phosphinodiselenoates are cumbersome and multistep in nature, relying on the handling of highly reactive and toxic phosphorus halides as well as air- and moisture-sensitive, flammable organometallic reagents [10].

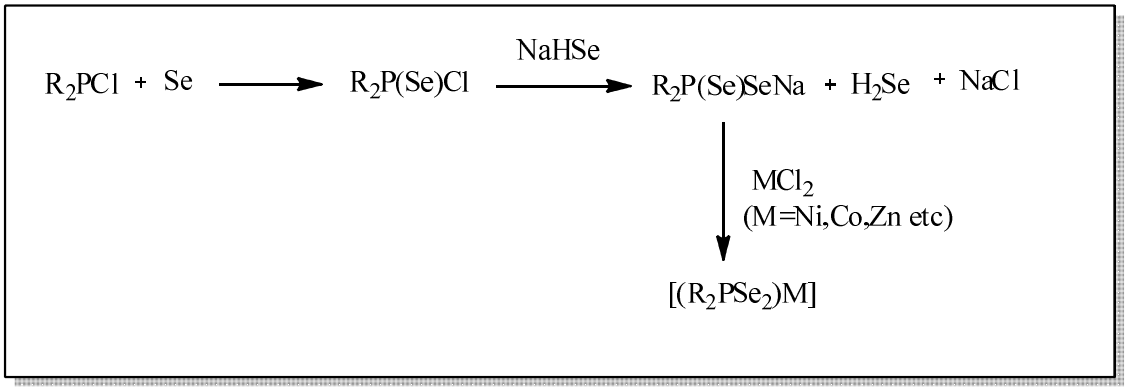

Fig 2.0- conventional route for synthesis of transition metal selenides complex.

Synthesis by using Et_3NH Based on R_2PCl, $HSiEt_3$, NEt_3, and Elemental Se.

In 1989, Du Mont and co-workers[11] demonstrated that elemental selenium can insert into the P–P bond of diphosphines, leading to the formation of bis(selenophosphoryl) selenides of the type $[R_2P(Se)]_2Se$. Building on this concept, Paul O'Brien[12] and colleagues later adapted a related strategy in 2007, exploiting the selenium-induced cleavage of P–Si bonds in diorgano(triethylsilyl)phosphines (R_2P-$SiEt_3$) to access previously unreported triethyl ammonium diselenophosphinate salts. Their synthetic protocol employed monochlorophosphines (R_2PCl), triethylsilane, triethylamine, and elemental selenium as the key reagents. Initially, treatment of the monochlorophosphines with triethylsilane in the presence of triethylamine generated the corresponding diorgano(triethylsilyl)phosphines. Subsequent prolonged reflux of these intermediates with elemental selenium and triethylamine in toluene afforded the desired triethylammonium diselenophosphinates has high isolated yields ranging from 80 to 89%.[12]

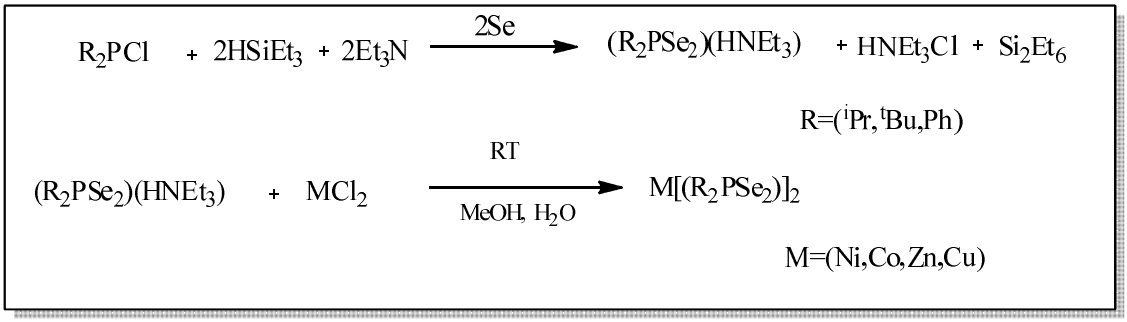

Fig3.0- Synthesis of alkali metal diselenophosphinates complex

IJARSCT
International Journal of Advanced Research in Science, Communication and Technology
International Open-Access, Double-Blind, Peer-Reviewed, Refereed, Multidisciplinary Online Journal
ISSN: 2581-9429
Volume 6, Issue 8, April 2026
Impact Factor: 8.2

Synthesis of Diselenophosphinate from Secondary Phosphines, Elemental Se and Alkali Metal Hydroxides

A widely used and practical strategy for preparing alkali metal phosphinodiselenoates is based on the treatment of secondary phosphine selenides with elemental selenium in the presence of an alkali metal hydroxide[13]. In contrast, the first time a direct three-component transformation involving a secondary phosphine, two molar equivalents of elemental selenium, and an alkali metal hydroxide. The successful implementation of this process is non-trivial, as secondary phosphines are well documented to preferentially react with two equivalents of selenium to produce bis(diorganoselenophosphoryl) selenides[14]. The one-pot synthesis is highly efficient and excellent yields can be obtained within a short time. The general synthesis of the alkali metal salt of diselenophosphinate is as follows and its further reacts with transition metal chloride to from metal selenides complex with its respective elements.

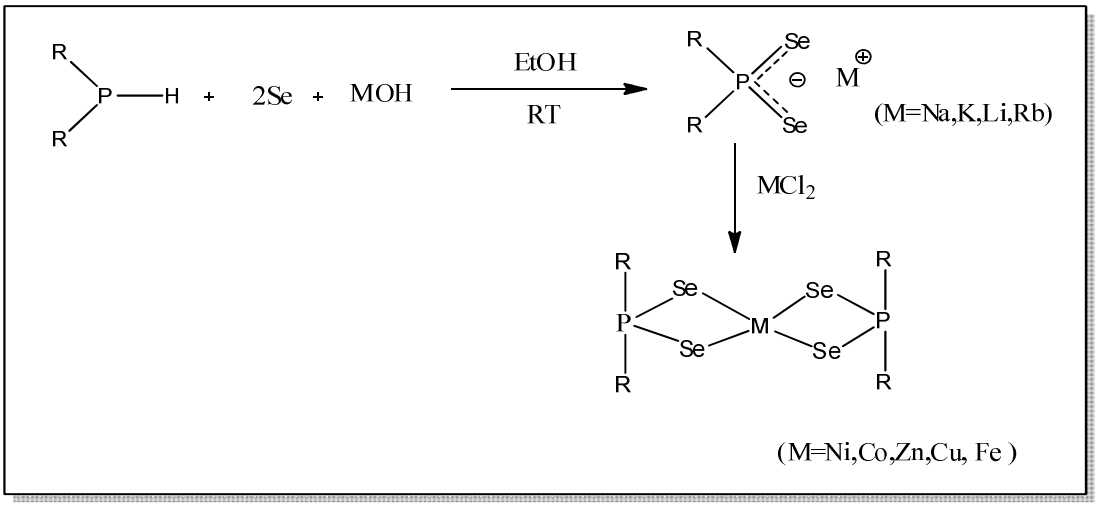

Fig4.0- The general synthesis of the alkali metal salt of diselenophosphinate is as follows

The single source precursor method has been proved to be highly effective for generating MC nanocrystalline materials if appropriate precursors can be chosen. The selected precursor must contain both the desired metal and corresponding chalcogen elements, which can decompose under a certain temperature to give MC compounds directly. By adjusting the ratios of the starting reagents (including precursors, ligands, and solvent) as well as the reaction temperature and reaction time, the size and morphology of the MC nanomaterials can be precisely controlled. Although the hot-injection and single-source precursor methods are very effective routes for the synthesis of high-quality MC nanomaterials, some disadvantages still exist. For example, the hot-injection method often involves complicated procedures and air-free manipulation, while the precursors used for the single-source precursor method are sometimes hard to be synthesized and are also limited in type.

Thin film deposition-

Chemcial vapour deposition-

The prepared ligand system demonstrates considerable flexibility, enabling the formation of a variety of diselenophosphinate coordination compounds [15]. These complexes have been examined as molecular precursors for the generation of nanoparticles through colloidal routes, as well as for thin film fabrication. The Silver diselenophosphinate and mixed thio-selenophosphinate complexes were also synthesized, and the solid-state structure of the tetranuclear species $[Ag(SSePiPr_2)]_4$ was established by single-crystal X-ray diffraction [16]. Structural analysis revealed a tetrahedral arrangement of four Ag(I) centers, each capped by four $SSePiPr_2$ ligands that coordinate through both sulfur and selenium donor atoms. Thermogravimetric studies showed that both complexes decompose in a single step within the 250–360 °C range. For the pure diseleno compound $[Ag(Se_2PiPr_2)]$, the residual mass exceeded that

IJARSCT
International Journal of Advanced Research in Science, Communication and Technology
International Open-Access, Double-Blind, Peer-Reviewed, Refereed, Multidisciplinary Online Journal
ISSN: 2581-9429 Volume 6, Issue 8, April 2026 Impact Factor: 8.2

expected for stoichiometric Ag_2Se, whereas the mixed thio-seleno analogue produced a residue consistent with the calculated value for Ag_2Se.

Thin films were deposited onto glass substrates via aerosol-assisted chemical vapour deposition (AA-CVD) at temperatures between 275 and 475°C. Films derived from the [Ag (Se_2PiPr_2)] precursor appeared grey, adhered well to the substrate, and exhibited diffraction patterns corresponding predominantly to orthorhombic Ag_2Se, along with minor contributions from an unidentified phase and a cubic Ag_2Se phase. Surface analysis showed irregularly shaped particles, and the films were slightly enriched in silver. In contrast, films obtained from the mixed chalcogen precursor displayed a comparable crystalline phase without detectable impurities and were marginally silver-deficient. Trace amounts of phosphorus were detected in films produced from both precursor systems.

Diselenophosphinate complexes have also proven to be promising single-source precursors for the controlled preparation of cobalt selenide or cobalt phosphide, achievable through both colloidal nanoparticle synthesis and AA-CVD deposition [17,18]. Cobalt derivatives such as $Co(Se_2PiPr_2)_2$, $Co(Se_2PPh_2)_2$, and $Co(Se_2PtBu_2)_2$ were evaluated for nanoparticle formation, while $Co(Se_2PiPr_2)_2$ was further utilized for thin film growth by AA-CVD. Similarly, nickel diselenophosphinate complexes $Ni(Se_2PiPr_2)_2$, $Ni(Se_2PtBu_2)_2$, and $Ni(Se_2PPh_2)_2$ have been employed for the deposition of nickel selenide and nickel phosphide nanoparticles and thin films via the same technique [48]. Crystallographic characterization of these nickel compounds confirmed a square-planar coordination geometry around the Ni(II) center, with each phosphorus atom adopting a tetrahedral configuration. Thin film deposition from the Co(Se2PiPr2)2 precursor was achieved on glass substrates via aerosol-assisted chemical vapor deposition (AA-CVD) at 450°C. No film growth occurred at lower temperatures. The deposited films consisted of a mixed phase containing cubic Co_9Se_8 and orthorhombic CoP, with surface morphologies characterized by irregular grains of varying dimensions.

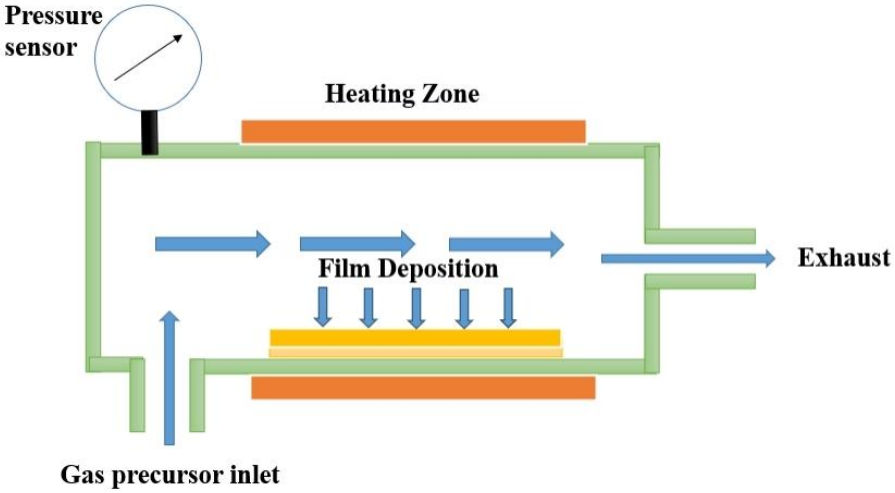

Fig 5.0- Chemical vapour deposition setup for TMC synthesis [77]

Hot injection method

The Cadmium selenide quantum dots (CdSe QDs) were synthesized using a continuous-flow reactor approach with [$Cd(Se_2PiPr_2)_2$] serving as the single-source precursor [19]. Key reaction variables including precursor concentration, reaction temperature (180–220°C), and residence time (4.2–16.8 s) were systematically optimized. Oleylamine was introduced into the system to prevent blockage of the microcapillary channels. Under controlled conditions, blue-emitting CdSe quantum dots of tunable size were obtained. Smaller nanocrystals, approximately 1.8–1.9 nm in diameter, formed at lower temperatures and shorter residence times, while increasing both parameters led to particle growth up to about 2.1 nm. A pronounced blue shift in the optical band gap was observed, consistent with strong quantum confinement effects. In addition, core shell CdSe/CdS nanostructures and CdSSe alloy nanoparticles were

IJARSCT
International Journal of Advanced Research in Science, Communication and Technology
International Open-Access, Double-Blind, Peer-Reviewed, Refereed, Multidisciplinary Online Journal
ISSN: 2581-9429 Volume 6, Issue 8, April 2026 Impact Factor: 8.2

prepared using an unsymmetrical cadmium dithiocarbamate complex as the sulfur source. Due to significant peak broadening, distinguishing between the hexagonal and cubic crystal phases of CdSe and CdSe/CdS nanocrystals proved challenging. Nevertheless, the formation of a CdS shell significantly improved the optical performance, with the photoluminescence quantum yield increasing from 7% for bare CdSe to 14% for CdSe/CdS core shell nanoparticles. The average size of the core shell particles was determined to be 4.0 ± 0.6 nm, while CdSSe alloy nanoparticles exhibited a larger size of approximately 5.0 ± 0.8 nm. The emission maximum of the alloy nanomaterials was shifted toward shorter wavelengths due to the incorporation of sulfur into the lattice. A complementary density functional theory (DFT) study by Donkor and co-workers examined the dissociation pathways and preferred decomposition products of the mixed-chalcogen cadmium complex $Cd[SSeP(C_6H_5)_2]_2$ [20]. Their theoretical analysis indicated that, based on product stability and activation energies, CdS formation is favored on the doublet potential energy surface, whereas CdSe formation is preferred when considering product stability, although CdS formation presents a lower activation barrier.

The colloidal synthesis of cobalt selenide ($CoSe_2$), cobalt precursors were injected into hot coordinating solvents such as hexadecylamine (HDA), trioctylphosphine oxide (TOPO), and mixed HDA/TOP or TOPO/TOP systems. When HDA or TOPO was used individually at 300°C, cobalt selenide nanocrystals were obtained; HDA favoured the formation of orthorhombic $CoSe_2$, while TOPO produced a mixture of orthorhombic and cubic phases. In contrast, cobalt phosphide formation required the presence of trioctylphosphine (TOP). No phosphide products were detected in the absence of TOP, at temperatures below 300°C, or for reaction times shorter than 60 min. Orthorhombic Co_2P was obtained after 60 min in TOPO/TOP or HDA/TOP mixtures at 300°C, whereas extending the reaction time to 150 min led to the formation of orthorhombic CoP. These observations suggest that TOP either supplies phosphorus directly or promotes precursor decomposition pathways that liberate phosphorus. Furthermore, single-crystal X-ray diffraction studies of copper diselenophosphinate revealed a tetrameric molecular structure, $Cu_4(Se_2PiPr_2)_4$, in which the ligands bridge between copper centers without exhibiting chelating coordination [21]. Copper selenide nanoparticles were subsequently synthesized through a hot-injection method using HDA/TOP solvent mixtures at reaction temperatures of 250 and 300°C [22,23].

Solvothermal method

In Based on the fact that the solvent properties, such as polarity, viscosity, and softness, have strong effects on the solubility and transport behavior of the precursors in liquid-based synthesis, which will control the reactivity, shapes, sizes, and phases of the final samples, different organic solvents can often be used as reaction media instead of water. This new strategy is known as the ‘‘solvothermal method’ ’Compared with the hydrothermal method, more solvents with special physicochemical properties can be chosen and the reaction temperature can be elevated to much higher values. By the solvothermal method, lots of MC nanocrystals with an elegant control of the size and shape distributions and also the crystallinity have been synthesized. Very few articles have been published on the solvothermal method.in below table we will explain different precursor and deposition techniques is used for deposition of metal selenides thin films.

IJARSCT
International Journal of Advanced Research in Science, Communication and Technology
International Open-Access, Double-Blind, Peer-Reviewed, Refereed, Multidisciplinary Online Journal
ISSN: 2581-9429
Volume 6, Issue 8, April 2026
Impact Factor: 8.2

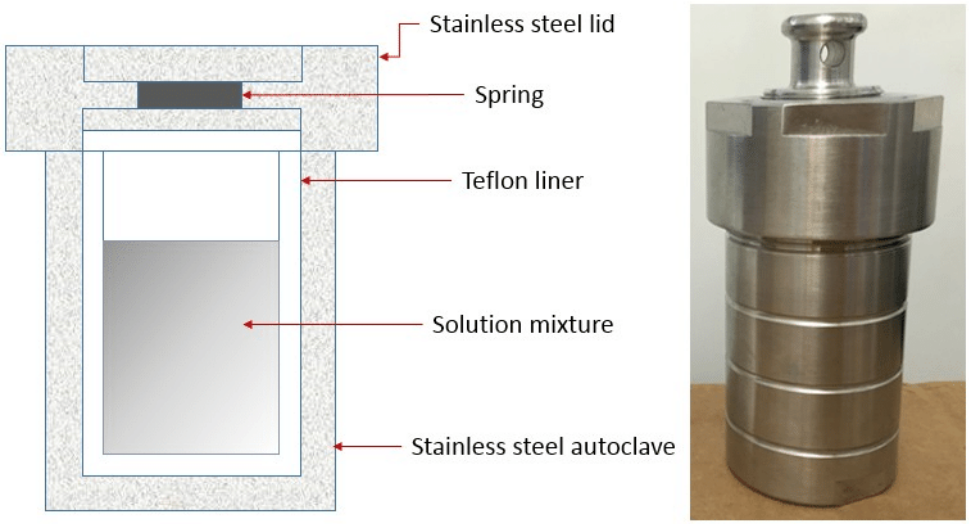

Fig 6.0- Solvothermal route of synthesis of TMC [78]

They few articles have been published on the solvothermal method. The below table we will explain different precursor and deposition techniques is used for deposition of metal selenides thin films

Precursor	Crystal structure elucidated	Material	Method	Substrate /Temperature	Ref
$Cd[(SeP^iPr_2)_2N]_2$	–	$CdSe/Cd_3P_2$	AACVD	Glass/475–525 C	[24]
$[MeCd(SeP^iPr_2)_2N]_2$	Yes	CdSe	LPCVD	Glass/450 C	[25]
$Cd[(SeP^iPr_2)_2N]_2$	–	CdSe	LPCVD	Glass/425–500 C	[26]
$Cd[(SePPh_2)_2N]_2$	–	CdSe	LPCVD	Glass/475–525 C	[17]
$Zn[(SeP^iPr_2)_2N]_2$ (R = Ph, ^{i}Pr)	Yes	ZnSe	LPCVD	Glass/400–525 C	[26,27]
$[Me_2M(SeP^iPr_2)_2N]$ (M = In, Ga)	Yes	M_2Se_3	LPCVD/AACVD	Glass/400–500 C	[28]
$In[(SeP^iPr_2)_2N]_2Cl$	–	In_2Se_3	LPCVD/AACVD	Glass/Si/GaAs/ 400–525 C	[29]
$Bi[(SePR_2)_2N]_3$ (R = Ph, ^{i}Pr)	Yes	Bi_2Se_3	LPCVD/AACVD	Glass/375–475 C	[30,31]
$Pb[(SePR_2)_2N]_2$ (R = Ph, ^{i}Pr)	–	PbSe	LPCVD/AACVD	Glass/400–450 C	[32,33]
$[Ag(^iPr_2P(X)NP(Se)^iPr_2)]_3$ (X = S, Se)	Yes	Ag_2Se	LPCVD/AACVD	Glass/325–475 C	[34,35]
$Fe[(SePR_2)_2N]_2$ (R = Ph, ^{i}Pr)	Yes	$Fe_7Se_8/FeSe_2$	AACVD	Glass/500–600 C	[36]
$Fe[(SeP^iPr_2)_2N]_2$	–	$FeSe/Fe_3Se_4$	Vapor transport	Glass/600–800 C	[37]
$Co[(SeP^iPr_2)_2N]_2$	–	$CoSe_2/CoP/CoP_2$	AACVD	Glass/375–525 C	[28]
$Pd[(^iPr_2PSe)_2N]_2$	–	$PdSe_2/Pd_{17}Se_{15}/Pd_4Se$	LPCVD	Glass/400–475 C	[38]
$Pt[(^iPr_2PSe)_2N]_2$	–	$PtSe_2$	LPCVD	Glass/400–475 C	[38]
$[Ag(XSeP^iPr_2)]_4$ (X = S, Se)	Yes	Ag_2Se	AACVD	Glass/275–475 C	[34]
$Co(Se_2P^iPr_2)_2$	–	Co_9Se_8/CoP	AACVD	Glass/450 C	[28]
$[Cu_4(Se_2P^iPr_2)_4]$	Yes	Cu2-xSe	AACVD	Glass/350–500 C	[39]

DOI: 10.48175/IJARSCT-33123

IJARSCT
International Journal of Advanced Research in Science, Communication and Technology
International Open-Access, Double-Blind, Peer-Reviewed, Refereed, Multidisciplinary Online Journal
ISSN: 2581-9429 Volume 6, Issue 8, April 2026 Impact Factor: 8.2

$In(^iPr_2PSe_2)_3$	Yes	In_2Se_3	AACVD	Glass/350–500 C	[39]
$Ni(Se_2P^iPr_2)_2$	Yes	$Ni_{0.85}Se$	AACVD	Glass/350–500 C	[38]
$Pb(SeSPPh_2)_2$	Yes	PbSe	AACVD	Glass/450–500 C	[40]
$[Sn(Se_2PPh_2)_2]$	–	$SnSe/Cu_3SnS_2$	AACVD	Glass/400–450 C	[41]
$M(Se_2P^iPr_2)_3$ (M = In, Ga) and $Cu(Se_2P^iPr_2)$	Yes	$CuMSe_2$	AACVD	Glass/350–500 C	[42]
$Zn(Se_2P^iPr_2)_2$	–	ZnSe	Solvothermal	HDA/300 C	[43]
$[Cu_4(Se_2P(O^iPr)_2)_4]$	Yes	Cu_2-xSe	MOCVD	Si/360 C	[44]
$[Cd(Se_2P^iPr_2)_2]$	–	CdSe	Flow reactor	OLA/180–220 C	[41]
$Co(Se_2PR_2)_2$ (R = Ph, ^{i}Pr, ^{t}Bu)	–	$CoSe_2$/CoP	Hot injection	HDA/TOPO/TOP/ 300 C	[43]
$[Cu_4(Se_2P^iPr_2)_4]$	yes	Cu_2-xSe	Hot injection	HDA/TOP/250–300 C	[44,45]
$In(Se_2P^iPr_2)_3$	yes	In_2Se_3	Hot injection	HDA/TOP/270 C	[44]
$Ni(Se_2PR_2)_2$ (R = Ph, ^{i}Pr, ^{t}Bu)	yes	$Ni_2P/Ni_{12}P_5/NiSe$	Hot injection	HDA/TOPO/TOP/ 280–330 C	[45]

Fig7.0- Molecular precursors used for the deposition of metal selenide thin films.

Applications of metal selenides-

Photovoltaics

The Dye-sensitized solar cells (DSSCs) are recognized as a representative class of third-generation photovoltaic technologies, characterized by their mesoporous electrode architecture and several appealing advantages, including low fabrication cost, environmental compatibility, simple processing, and comparatively high power conversion efficiency (PCE). Over the past two decades, extensive research efforts have been devoted to enhancing the photovoltaic efficiency of DSSCs while simultaneously reducing manufacturing expenses [46]. In comparative studies of counter-electrode (CE) materials, DSSCs employing $Co_{0.85}Se$ Nano sheet-based CEs achieved a PCE of 9.40%, which surpasses those obtained with $Ni_{0.85}Se$ nanoparticle CEs (8.32%) and conventional Pt CEs (8.64%). Because $Co_{0.85}Se$ and $Ni_{0.85}Se$ exhibit similar intrinsic catalytic activity when prepared with identical morphologies, the observed performance disparity between $Co_{0.85}Se$ Nano sheets and $Ni_{0.85}Se$ nanoparticles can be primarily ascribed to differences in morphology rather than the metal species itself. Morphological characteristics also play a crucial role in determining electrochemical durability. Nano sheet structures provide a larger interfacial contact area and stronger adhesion to fluorine-doped tin oxide (FTO) substrates compared with nanoparticle films, resulting in improved electrochemical stability for $Co_{0.85}Se$ Nano sheet-based CEs. Furthermore, the increased catalyst–electrolyte contact area associated with Nano sheet morphologies effectively reduces Nernst diffusion impedance relative to nanoparticle-based counterparts.

Another notable advantage of in situ–grown $Co_{0.85}Se$ Nano sheet and $Ni_{0.85}Se$ nanoparticle counter electrodes is their high optical transparency, exceeding 85% in the visible wavelength range [47]. This transparency arises from the fact that excellent catalytic performance can be achieved with very low material loadings, typically below 10 μg cm^{-2}. When a reflective mirror is placed beneath a transparent $Ni_{0.85}Se$ nanoparticle CE, the device efficiency is further enhanced, as transmitted light from the photo anode can be reflected back into the active layer. Owing to this high transparency, metal selenide-based counter electrodes are particularly well suited for bifacial DSSC configurations.[48] Building on this advantage, Tang and co-workers developed a series of transparent metal selenide counter electrodes using an in situ growth strategy for bifacial DSSCs. Devices incorporating transparent $Co_{0.85}Se$, $Ru_{0.33}Se$, FeSe, and $Ni_{0.85}Se$ counter electrodes not only delivered high efficiencies under front-side illumination but also maintained respectable PCE values under rear-side illumination. These bifacial DSSCs demonstrate the capability of harvesting

IJARSCT
International Journal of Advanced Research in Science, Communication and Technology
International Open-Access, Double-Blind, Peer-Reviewed, Refereed, Multidisciplinary Online Journal
ISSN: 2581-9429
Volume 6, Issue 8, April 2026
Impact Factor: 8.2

solar energy effectively from either side of the device, or simultaneously from both sides, highlighting their potential for enhanced energy generation in practical applications.[49,50].

A wide range of metal selenides containing different metal ions and compositional ratios has been developed, most commonly through hydrothermal or solvothermal techniques. By altering the type of metal precursor and adjusting the metal-to-selenium ratio, materials with varied stoichiometry's can be obtained. Furthermore, parameters such as solvent choice and the presence of surfactants play a decisive role in tailoring crystal growth and controlling morphology. Several fabrication routes have been employed to construct metal selenide counter electrodes (CEs). Among them, the in situ growth approach stands out because it enables uniform coverage on the conductive substrate, enhances interfacial adhesion, and maximizes the exposure of active catalytic sites. Beyond their strong electrocatalytic performance, metal selenide Nano sheets prepared through in situ strategies are also promising for high-efficiency fiber-shaped DSSCs. Their excellent optical transparency further allows their use in bifacial DSSCs, where light can be effectively utilized from both the photo anode side and the counter electrode side. Owing to their low cost, good durability, and high catalytic efficiency, metal selenides are emerging as competitive alternatives to conventional CE materials for large-scale deployment. Although substantial progress has been achieved in applying metal selenides as counter electrodes in DSSCs, several important issues remain unresolved. The fundamental catalytic mechanism of these materials is not yet fully clarified, and a deeper understanding would provide valuable guidance for the rational design of more efficient compositions. Additionally, the influence of stoichiometric variation on catalytic activity deserves systematic investigation. Such studies require precise synthetic control to maintain consistent morphology while varying composition, ensuring that performance differences can be accurately attributed to changes in chemical ratio rather than structural effects [49].

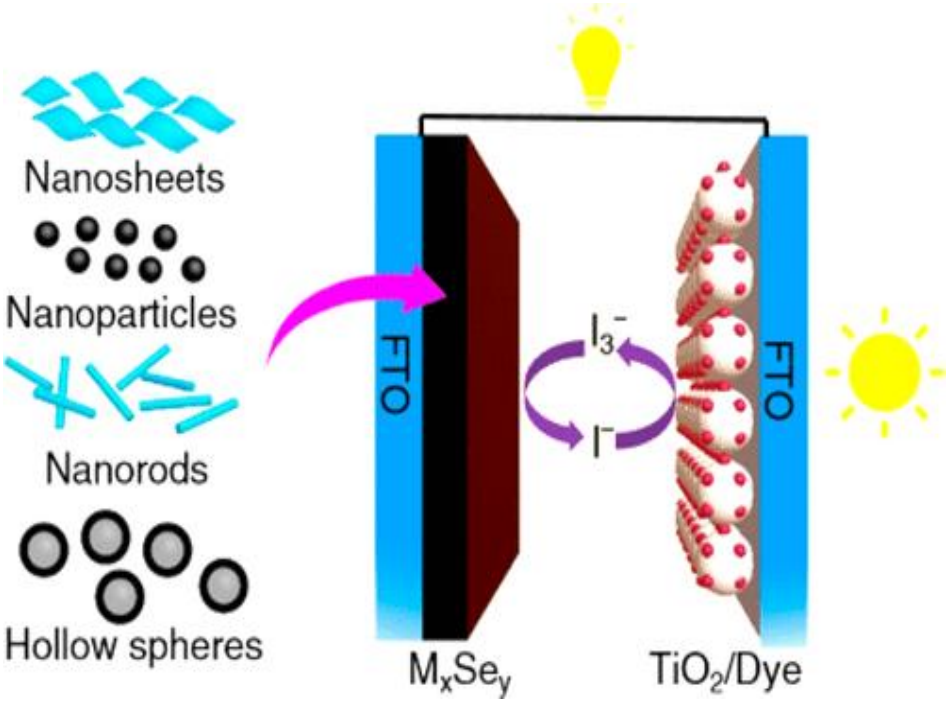

Fig8.0-Metal Selenides as Efficient Counter Electrodes for Dye-Sensitized Solar Cells [79]

Batteries-

The graphite remains the most widely used anode material in lithium-ion batteries because of its stable and flat voltage profile, high coulombic efficiency, and reliable long-term cycling stability. Despite these advantages, graphite suffers

IJARSCT
International Journal of Advanced Research in Science, Communication and Technology
International Open-Access, Double-Blind, Peer-Reviewed, Refereed, Multidisciplinary Online Journal
ISSN: 2581-9429 Volume 6, Issue 8, April 2026 Impact Factor: 8.2

from inherent limitations, including a comparatively low theoretical capacity and sluggish lithium-ion transport kinetics. These shortcomings have motivated extensive research aimed at identifying alternative anode materials with improved performance. Among the various candidates explored, transition metal selenides have attracted attention due to their potential to deliver higher specific capacities than conventional graphite. Owing to their semiconducting nature, with band gap energies typically ranging from approximately 0.15 to 2.7 eV, these materials have been investigated for lithium storage applications since the 1970s. Progress in synthetic strategies and advancements in lithium battery technology have further stimulated interest in employing transition metal selenides as anode materials.[51].

VSe_2 is a member of the layered transition metal dichalcogenide family, whose structure enables the reversible insertion and extraction of lithium ions between adjacent layers. In its ultrathin nanosheet form, VSe_2 exhibits metallic behavior and high electrical conductivity, features that are advantageous for electrochemical energy-storage applications. These properties position VSe_2 as a promising candidate for use in lithium batteries.[52] The lithium- and sodium-ion intercalation behavior of layered $MoSe_2$[53,54]; however, at that stage, the electrochemical performance of $MoSe_2$-based electrodes in battery systems was not systematically evaluated. In more recent work, highly ordered mesoporous crystalline $MoSe_2$ has been successfully fabricated using a nanocasting strategy with SBA-15 as a rigid template. The resulting material exhibits a well-defined hexagonal mesostructure along with a rod-like morphology. When employed as an anode material in lithium-ion batteries, the mesoporous $MoSe_2$ delivered a stable and reversible lithium-storage capacity of approximately 630 mAh g^{-1}, maintaining this value over 35 charge–discharge cycles without significant capacity fading. Moreover, this mesoporous $MoSe_2$ anode demonstrated markedly improved rate capability compared with its mesoporous MoS_2 counterpart, underscoring its suitability for high-power lithium-ion battery applications. In a related study, WSe_2 with a band gap of about 1.2 eV and an electrical conductivity of 6×10^{-1} cm^{-1} using the same SBA-15 templating approach. Lithium-ion batteries incorporating mesoporous WSe_2 as the anode exhibited initial discharge and charge capacities of 762 and 555 mAh g^{-1}, respectively, exceeding the theoretical capacity of WSe_2 at a rate of 0.1 C. Comparable behavior has also been reported for $MoSe_2$ and MoS_2 systems, which is generally attributed to additional lithium storage at interfacial sites within the mesoporous architecture.[55].

Nickel and selenium are capable of forming a range of selenide phases, including non-stoichiometric compositions, and their physical as well as electrochemical properties are strongly influenced by variations in composition, crystal structure, and morphology. Among these phases, penroseite-type $NiSe_2$ adopts a cubic pyrite structure and behaves as a Pauli paramagnetic metal, exhibiting a low electrical resistivity (below 10^{-3} Ω·cm). Such high electrical conductivity makes it attractive for use as an electrode material in rechargeable lithium batteries. $NiSe_2$ thin films and their lithium-storage performance was systematically evaluated. The initial discharge capacity reached 467.5 mAh g^{-1} but declined to 313 mAh g^{-1} within the first three cycles, corresponding to a retention of approximately 67% of the original capacity. After this early stabilization phase, the electrode demonstrated steady cycling behavior, maintaining a capacity of about 314.9 mAh g^{-1} even after 200 cycles. The lithium insertion and extraction mechanism in the Li/$NiSe_2$ system was found to be comparable to that observed in Li/VSe_2 cells[56]. Because nickel and selenium possess similar electronegativity values and compatible electronic configurations, they readily combine to generate multiple stoichiometric and structural variants. These differences in phase composition and crystal arrangement significantly influence the electronic structure and, consequently, the electrochemical characteristics of the resulting materials.[57].

Thin films of $CuSe_2$, CuSe, and Cu_2Se were fabricated using a pulsed laser deposition (PLD) technique, in which copper and selenium were ablated from mixed targets. Owing to differences in chemical composition and crystal structure, these three copper selenide phases displayed distinct electrochemical behaviors when evaluated as lithium battery electrodes. Within a voltage window of 1.0–2.5 V, the $CuSe_2$/Li, CuSe/Li, and Cu_2Se/Li cells delivered reversible capacities of 201.7, 258.4, and 210.2 mAh g^{-1}, respectively. Among them, Cu_2Se demonstrated the most stable cycling performance, maintaining 177.7 mAh g^{-1} after 100 cycles, which corresponds to approximately 73% of its initial discharge capacity. The superior stability of the Cu_2Se/Li system is attributed to a reversible structural transformation between Cu_2Se and Cu during cycling. Because Cu_2Se and Li_2Se share similar lattice characteristics, volume expansion and structural distortion are minimized, thereby enhancing durability.[58]

IJARSCT
International Journal of Advanced Research in Science, Communication and Technology
International Open-Access, Double-Blind, Peer-Reviewed, Refereed, Multidisciplinary Online Journal
ISSN: 2581-9429 Volume 6, Issue 8, April 2026 Impact Factor: 8.2

In contrast, CuSe/Li and $CuSe_2$/Li cells exhibited improved cycling stability when operated within a narrower voltage range of 1.8–2.5 V. Under these conditions, discharge capacities of 118.9 and 196.6 mAh g^{-1}, respectively, were preserved after 100 cycles [59]. The comparable electronegativity and closely related electronic configurations, nickel and selenium can combine to form selenides with a wide range of stoichiometries and structural arrangements, which in turn strongly influence their electronic behavior. Using this compositional flexibility, Mi and co-workers prepared NiSe with distinct morphologies via a hydrothermal method employing nickel foam and selenium powder as precursors. When synthesized at 140 °C, the NiSe initially displayed a layered morphology that gradually evolved into a three-dimensional, hierarchically organized tubular structure as the reaction duration increased. Lithium-ion batteries assembled with these structurally evolved NiSe electrodes exhibited a notable rise in initial discharge capacity, increasing from 295.3 to 410.7 mAh g^{-1}, with a characteristic voltage plateau around 1.40 V. In contrast, NiSe produced at a higher temperature of 180 °C for 24 hours formed tubular architectures composed of aggregated nanoparticles. This material delivered a lower initial capacity of 306.5 mAh g^{-1} and showed a smoother discharge plateau centered near 1.90 V. These findings underscore the decisive influence of electrode architecture on electrochemical performance. Nevertheless, further investigation is required to fully clarify the lithium-storage mechanisms and long-term cycling behavior of NiSe when used as an anode material.[57]

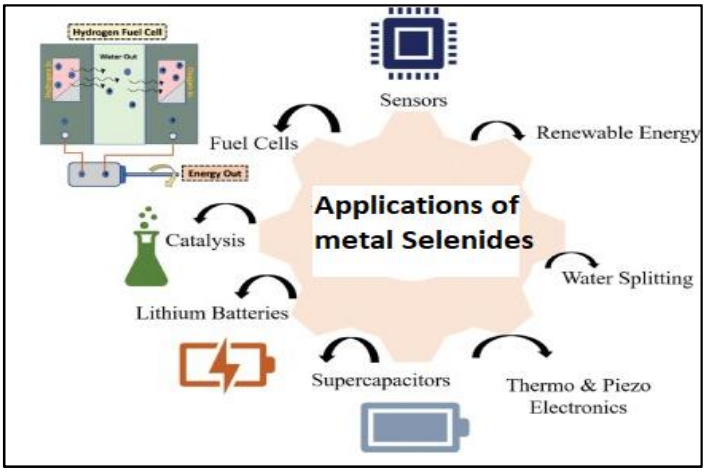

Fig 9.0- Applications of transition metal selenides

3) Supercapacitor-

Supercapacitors represent a distinct class of electrochemical energy-storage systems known for their ability to provide exceptionally high power output; however, their practical application is often constrained by relatively low energy density. As a result, considerable research attention has been directed toward strategies aimed at enhancing their energy-storage capability. Among the various approaches, expanding the operating voltage window of electrode materials has proven particularly effective, since the energy density of a supercapacitor is intrinsically dependent on both its capacitance and the applied potential range. The electrochemical performance of supercapacitors is strongly dependent on the intrinsic properties and structural design of the electrode materials. In particular, electrodes possessing hierarchical, tubular, or layered nanostructures can effectively accelerate charge transfer and ion diffusion processes, thereby improving power density and maintaining long-term cycling stability. Commonly used electrode materials include carbon-based materials, metal oxides, and electrically conducting polymers. Nevertheless, identifying and developing new electrode materials remains a crucial and ongoing challenge for achieving further performance enhancement.

In recent years, nanostructured transition metal selenides have attracted growing interest as promising supercapacitor electrode materials. This interest arises from their graphene-like layered frameworks combined with

IJARSCT
International Journal of Advanced Research in Science, Communication and Technology
International Open-Access, Double-Blind, Peer-Reviewed, Refereed, Multidisciplinary Online Journal
ISSN: 2581-9429 Volume 6, Issue 8, April 2026 Impact Factor: 8.2

favourable electrical conductivity and mechanical robustness, making them especially appealing for next-generation supercapacitors, particularly flexible and all-solid-state energy-storage devices.[60].As electrode materials for supercapacitors, $Co_{0.85}Se$ nanotubes have demonstrated remarkable electrochemical behaviour, delivering a specific capacitance of 238 F g^{-1} at 1 A g^{-1} along with excellent cycling durability, retaining 90.3% of their initial capacitance after 1900 charge–discharge cycles.[60]

Subsequently, Banerjee and co-workers developed an advanced electrode architecture based on $Co_{0.85}Se$ hollow nanowire (HNW) arrays. These structures were obtained through a wet-chemical hydrothermal selenization process, where cobalt hydroxyl carbonate nanowires were first grown on conductive carbon fiber paper and then converted into the selenide phase. The resulting hollow nanowires exhibited pronounced pseudo capacitive characteristics, achieving a very high gravimetric capacitance of 674 F g^{-1} at 1.48 A g^{-1} and maintaining 444 F g^{-1} even at an elevated current density of 11 A g^{-1}. Moreover, the electrode showed strong capacitance retention and excellent long-term stability. When assembled into an asymmetric full-cell device using $Co_{0.85}Se$ hollow nanowires as the positive electrode and activated carbon as the negative electrode, the system delivered an energy density of 6×10^{-5} Wh cm^{-2} together with good cycling performance, preserving 94% of its capacitance after 1000 cycles. More recently, the growth of hierarchical $CoSe_2$ nanostructures directly on conductive carbon fabrics via a simple two-step fabrication strategy, achieving strong interfacial adhesion and improved electrochemical performance.[61].the obtained material delivered a high areal specific capacitance of 332 mF cm^{-2} at a current density of 1 mA cm^{-2} and maintained approximately 95.4% of its initial capacitance after 5000 charge–discharge cycles, indicating excellent cycling durability. Furthermore, flexible all-solid-state asymmetric supercapacitor devices constructed using the hierarchical $CoSe_2$ electrode as the negative electrode and MnO_2 nanowires as the positive electrode exhibited an expanded operating voltage window of 1.6 V. These devices achieved a high energy density of 0.588 mWh cm^{-3} at a corresponding power density of 0.282 W cm^{-3}, while also demonstrating outstanding mechanical robustness and flexibility.[62]

Nest-like $NiSe_2$ composite electrodes have been developed as promising candidates for advanced supercapacitor applications. In this study, a three-dimensional hierarchical $NiSe_2$ framework composed of interconnected nanorods was first constructed. This architecture was subsequently employed as a sacrificial template, and through a controlled partial ion-exchange process, it was converted into a NiSe2 composite structure. The resulting three-dimensional nest-like $NiSe_2$ electrode demonstrated outstanding rate capability along with a high specific capacity of 1412Fg^{-1} at a current density of 0.5Ag^{-1}. This strategy where selected ions are deliberately incorporated into a pre-formed parent structure to generate tailored compositions offers a versatile route for tuning material properties. Importantly, such an approach is not limited to metal selenides and can be extended to other material systems to enhance electrochemical characteristics and overall device performance [63]. Despite the extensive body of work devoted to the synthesis and electrochemical applications of transition metal selenides, their intrinsic electrochemical behaviour has received comparatively limited attention. Then systematically investigated the influence of lithium-ion intercalation exfoliation on the charge-transfer properties of transition metal diselenides, specifically $MoSe_2$ and WSe_2, using electrochemical impedance spectroscopy. Their study revealed that these selenide-based transition metal systems exhibit more rapid heterogeneous electron-transfer kinetics than their sulfide counterparts, such as MoS_2 and WS_2, when evaluated with the $[Fe(CN)_6]^{3-/4-}$ redox couple. Furthermore, electrochemical activation was shown to significantly reduce the charge-transfer resistance of the selenide materials. These findings offer valuable insight into the fundamental electrochemical nature of transition metal selenides and highlight their strong potential as alternative electrode materials for electrochemical energy-storage applications.[64]

Electrocatalysis-

In the initial phase of research on selenide electrocatalysts for the hydrogen evolution reaction (HER), nickel- and cobalt-based materials attracted significant interest due to their favourable electronic structures and catalytic potential. As early as 2015, [65] the in-situ growth of NiSe nanowires directly on nickel foam using NaHSe as the selenium source through a facile hydrothermal approach. The resulting three-dimensional NiSe/NF electrode exhibited excellent

IJARSCT
International Journal of Advanced Research in Science, Communication and Technology
International Open-Access, Double-Blind, Peer-Reviewed, Refereed, Multidisciplinary Online Journal
ISSN: 2581-9429 Volume 6, Issue 8, April 2026 Impact Factor: 8.2

electrocatalytic performance, enabling overall water splitting to reach a current density of 10 mA cm^{-2} at a cell voltage of 1.63 V. The Nickel is characterized by its $3d^8 4s^2$ electronic configuration and a relatively small electronegativity difference with selenium, allowing the formation of multiple stoichiometric nickel selenide phases. Consequently, a variety of compounds such as NiXSe ($0.5 \leq x \leq 1$), $NiSe_2$[66,67,68], and Ni_3Se_2 have been successfully synthesized and investigated. Electrochemical evaluations revealed that $NiSe_2$ delivers a notably lower overpo tential of approximately 156 mV at 10 mA cm^{-2} in 0.5 M H_2SO_4 [66] when compared with its sulfur and tellurium analogues, namely NiS_2 and $NiTe_2$. Further enhancement of catalytic activity was achieved by simultaneously introducing phosphorus dopants and selenium vacancies into $NiSe_2$ nanosheet arrays. Argon plasma treatment was shown to increase the density of active sites and improve electrical conductivity, thereby significantly boosting intrinsic HER activity.

Importantly, the studies have demonstrated that dynamic phase evolution can also contribute to enhance HER performance. During electrochemical operation, cubic $NiSe_2$ undergoes an in-situ transformation into hexagonal NiSe. This phase transition is driven by charge accumulation on Se–Se dimers under cathodic polarization, which weakens the Se–Se bonds and induces lattice contraction. The transformation occurs heterogeneously across the material, generating abundant phase boundaries that facilitate charge transfer. Accompanying electron redistribution from selenium to nickel leads to improved electrical conductivity and a favourable shift of the d-band center, ultimately rendering the newly formed NiSe phase the true catalytically active species. Although the preparation of phase-pure nickel selenides remains challenging, constructing multiphase nickel selenide composites through simple synthetic routes has emerged as an effective interface-engineering strategy. Various heterostructured systems, including $NiSe/Ni_{0.85}$[69]Se nanoarrays, Ni_3Se_2/NiSe nanorods[70], and $NiSe/Ni_3Se_2$ nanowires[71,72], have demonstrated superior HER activity due to synergistic interfacial effects. In particular, lattice-matched $NiP_2/NiSe_2$ heterostructures were rationally designed to promote electronic redistribution at the interface. Density functional theory calculations indicated that strong electronic coupling between NiP_2 and $NiSe_2$ optimizes hydrogen adsorption energetics. As a result, these heterostructures exhibit excellent HER performance in alkaline media, requiring an overpotential as low as 66 mV to reach 10 mA cm^{-2} in 1M KOH.

Cobalt-based selenides have also emerged as promising HER electrocatalysts. In cubic $CoSe_2$, elongation of the Co–Se bond leads to increased electron density localized on selenium atoms, which facilitates the adsorption of hydrogen intermediates and promotes H_2 formation [73]. The catalytic activity of $CoSe_2$ can be further improved through heteroatom doping. Sulfur incorporation effectively tunes the hydrogen adsorption free energy toward thermoneutral values while simultaneously lowering the kinetic barrier of the rate-determining step. Additionally, phosphorus doping induces a structural phase transition from the cubic to the orthorhombic phase. When the phosphorus content reaches approximately 8wt%, orthorhombic $CoSe_2$ exhibits outstanding HER performance, achieving an overpotential of 104 mV and an onset potential as low as 31 mV at a current density of 10 mA cm^{-2} in 1M KOH.[74] Beyond single-phase materials, cobalt selenide heterostructures have shown considerable promise. Mixed-phase $CoSe/Co_9Se_8$ three-dimensional electrodes were fabricated via one-step calcination of cobalt foil with selenium powder in vacuum-sealed ampoules. The oxidation state of cobalt, which can be modulated by controlling the Co/Se ratio, plays a critical role in determining electrocatalytic behaviour. Mechanistic investigations revealed that cobalt species with lower oxidation states favor hydrogen evolution, whereas higher oxidation states are more conducive to oxygen evolution reactions.[75,76]. To address the limitations encountered in electrochemical energy-storage systems, it is essential to develop new categories of transition metal selenides (TMS) with improved performance characteristics. One effective strategy involves constructing nanostructured composites by integrating TMS with other functional materials. Such hybrid designs offer a practical pathway to satisfy the increasing demands of next-generation energy-storage technologies. The successful utilization of materials such as $CoSe_2$, $NiSe_2$, and ZnSe in lithium-ion batteries highlights the advantages of this approach. By carefully selecting and combining different components, TMS-based nanocomposites can harness the complementary strengths of each constituent, thereby enhancing overall electrochemical behaviour.

DOI: 10.48175/IJARSCT-33123

IJARSCT
International Journal of Advanced Research in Science, Communication and Technology
International Open-Access, Double-Blind, Peer-Reviewed, Refereed, Multidisciplinary Online Journal
ISSN: 2581-9429
Volume 6, Issue 8, April 2026
Impact Factor: 8.2

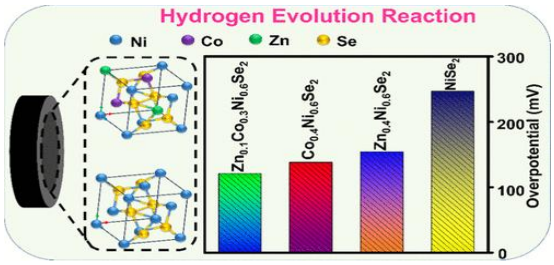

Fig10.0 -Electrocatalysts for the Hydrogen Evolution Reaction of TMS[80]

However, although synergistic improvements have been observed, the fundamental mechanisms responsible for these cooperative effects remain insufficiently understood and warrant further investigation. Particular emphasis should be placed on electrode architecture, as structural design plays a crucial role in facilitating ion transport both within the active material and across the electrode electrolyte interface. Innovative electrode configurations must therefore be engineered to ensure long-term cycling stability and reliable device operation. The Advances in nanotechnology are expected to open new avenues for the scalable and cost-effective production of nanostructured transition metal selenides. Achieving this goal requires a comprehensive understanding of crystal growth mechanisms, the influence of synthesis parameters on structural evolution, and the relationship between structure and electrochemical properties. Such insights will enable the rational design and fabrication of transition metal selenides with tailored characteristics suited for high-performance energy-storage applications.

2. Conclusion and future Perspective-

Transition metal selenide (TMS) nanomaterials have emerged as highly promising electrode candidates for advanced electrochemical energy storage systems including batteries, Photovolatics, supercapacitors and electrocatalysis. Their distinctive physicochemical characteristics such as rich redox activity and structural diversity enable high electrochemical performance. Notably, parameters such as specific capacity, rate performance, and long-term cycling stability can be significantly improved through rational structural engineering and by constructing hybrid composites with conductive nanomaterials like graphene and other carbonaceous frameworks. The compositional tunability of TMS further enables the development of next-generation, high-performance energy storage devices. Despite these advantages, several challenges still limit the practical deployment of transition metal selenides. One major issue is their relatively low intrinsic electrical conductivity. Elemental doping during material synthesis has been proposed as an effective strategy to enhance charge transport properties; however, systematic investigations are still required to optimize dopant type, concentration, and distribution. In addition, cycling durability remains a concern, as repeated ion insertion and extraction often induce substantial volume changes, leading to structural degradation and capacity fading.

To address these limitations, the design of novel TMS compositions and architectures is essential. Constructing nanostructured composites by integrating TMSs with complementary functional materials represents a particularly effective approach. For example, incorporating selenides such as $CoSe_2$, $NiSe_2$, and ZnSe into battery systems has demonstrated that synergistic interactions within composite structures can improve electrochemical stability and overall performance. Nevertheless, the underlying mechanisms governing these synergistic effects are not yet fully understood and warrant further investigation. Electrode architecture also plays a decisive role in determining ion diffusion kinetics and interfacial charge transfer between the electrode and electrolyte. Innovative structural designs are therefore required to facilitate efficient ion transport while maintaining mechanical integrity during prolonged cycling. Advances in nanotechnology provide substantial opportunities for scalable and cost-effective fabrication of nanostructured transition metal selenides. However, achieving this goal demands a comprehensive understanding of growth mechanisms, synthesis–structure relationships, and how processing parameters influence the final electrochemical

IJARSCT
International Journal of Advanced Research in Science, Communication and Technology
International Open-Access, Double-Blind, Peer-Reviewed, Refereed, Multidisciplinary Online Journal
ISSN: 2581-9429 Volume 6, Issue 8, April 2026 Impact Factor: 8.2

properties. Such insights will enable the rational design of tailored TMS materials with optimized performance for future energy storage applications.

Acknowledgments

This work was supported by Department of Chemistry, Ecole Centrale School of Engineering, Mahindra University, Hyderabad, Telangana, India

Conflict of Interest

The authors declare no conflict of interest.

REFERENCES

[1] L. Capuano, in US Energy Information Administration, 2020, vol. 2020, pp. 1–7.
[2] P.J. Heard, Prog. Inorg. Chem. 53 (2005) 1–69.
[3] E.R. Tiekink, I. Haiduc, Prog. Inorg. Chem 54 (2005) 127–319.
[4] I. Haiduc, D.B. Sowerby, S.-F. Lu, Polyhedron 14 (1995) 3389–3472.
[5] J.J. Vittal, M.T. Ng, Acc. Chem. Res. 39 (2006) 869–877.
[6] M. Afzaal, M.A. Malik, P. O'Brien, J. Mater. Chem. 20 (2010) 4031–4040.
[7] W. Kuchen, B. Knop, Angew. Chem. Int. Ed. 4 (1965) 244–245.
[8] A.V. Artem'ev, N.K. Gusarova, S.F. Malysheva, B.A. Trofimov, Org. Prep. Proced. Int. 43 (2011) 381–449.
[9] A.V. Artem'ev, S.F. Malysheva, N.K. Gusarova, B.A. Trofimov, Synthesis (2010) 2463–2467.
[10] Kuchen, W.; Metten, J.; Judat, A. Chem. Ber. 1964, 97, 2306. (b) Kuchen, W.; Knop, B. Angew. Chem., Int. Ed. Engl. 1965, 4, 244. (c) Kuchen, W.; Hertel, H. Angew. Chem., Int. Ed. Engl. 1969, 8, 89. (d) Davies, R. P. Martinelli, M. G. Inorg. Chem. 2002, 41, 348.
[11] W.-W. DuMont, R. Hensel,W. McFarlane, I. J. Colquhoun, M. L. Ziegler and O. Serhadli, Chem. Ber., (1989)122, 37
[12] C. Q. Nguyen, M. Afzaal, M. A. Malik, M. Helliwell, J. Raftery and P. O'Brien, J. Organomet. Chem., (2007) 692, 2669 (2007).
[13] Trofimov, B. A Artem'ev, A. V.Malysheva, S. F Gusarova, N. K. J. Organomet. Chem. 2009, 694, 4116.
[14] Artem'ev, A. V. Gusarova, N. K. Malysheva, S. F.Ushakov, I. A Trofimov, B. A. Tetrahedron Lett. 2010, 51, 2141
[15] C.Q. Nguyen, A. Adeogun, M. Afzaal, M.A. Malik, P. O'Brien, Chem. Commun. (2006) 2182–2184.
[16]C.Q. Nguyen, M.A. Malik, P. O'Brien, J. Raftery, J. Mater. Chem. 19 (2009) 419–427.
[17]A. Panneerselvam, C.Q. Nguyen, J. Waters, M.A. Malik, P. O'Brien, J. Raftery, M. Helliwell, Dalton Trans. (2008) 4499–4506.
[18]W. Maneeprakorn, M.A. Malik, P. O'Brien, J. Mater. Chem. 20 (2010) 2329– 2335.
[19]A.L. Abdelhady, M. Afzaal, M.A. Malik, P. O'Brien, J. Mater. Chem. 21 (2011) 18768–18775.
[20] F. Opoku, N.K. Asare-Donkor, A.A. Adimado, Chem. Central J. 10 (2016) 4.
[21] C.Q. Nguyen, A. Adeogun, M. Afzaal, M.A. Malik, P. O'Brien, Chem. Commun. (2006) 2182–2184.
[22]S.N. Malik, M. Akhtar, N. Revaprasadu, A.Q. Malik, M.A. Malik, IOP Conference Series: Materials Science and Engineering, IOP Publishing, 2014, p. 012019.
[23]S.N. Malik, H. Ahmed, M. Shahid, N. Haider, M. Malik, P. O'Brien, Applied sciences and technology (IBCAST), in: 2013 10th International Bhurban Conference on, IEEE, 2013, pp. 39–42.
[24]T. Oyetunde, M. Afzaal, M.A. Vincent, P. O'Brien, Dalton Trans. 45 (2016) 18603–18609.
[25]M. Afzaal, D. Crouch, M.A. Malik, M. Motevalli, P. O'Brien, J.-H. Park, J. Mater.
Chem. 13 (2003) 639–640.

IJARSCT
International Journal of Advanced Research in Science, Communication and Technology
International Open-Access, Double-Blind, Peer-Reviewed, Refereed, Multidisciplinary Online Journal
ISSN: 2581-9429 Volume 6, Issue 8, April 2026 Impact Factor: 8.2

[26]M. Afzaal, D. Crouch, M.A. Malik, M. Motevalli, P. O'Brien, J.H. Park, J.D. Woollins, Eur. J. Inorg. Chem.(2004) 171–177.
[27]M. Afzaal, S.M. Aucott, D. Crouch, P. O'Brien, J.D. Woollins, J.H. Park, Chem. Vap. Deposition 8 (2002) 187–189.
[28]J.-H. Park, M. Afzaal, M. Helliwell, M.A. Malik, P. O'Brien, J. Raftery, Chem. Mater. 15 (2003) 4205–4210.
[29]M. Afzaal, D. Crouch, P. O'Brien, Mater. Sci. Eng. B 116 (2005) 391–394.
[30]D.J. Crouch, M. Helliwell, P. O'Brien, J.-H. Park, J. Waters, D.J. Williams, Dalton Trans. (2003) 1500–1504.
[31]J. Waters, D. Crouch, J. Raftery, P. O'Brien, Chem. Mater. 16 (2004) 3289–3298.
[32]N.O. Boadi, P.D. McNaughter, M. Helliwell, M.A. Malik, J.A. Awudza, P. O'Brien, Inorg. Chim. Acta 453 (2016) 439–442.
[33]M. Afzaal, K. Ellwood, N.L. Pickett, P. O'Brien, J. Raftery, J. Waters, J. Mater. Chem. 14 (2004) 1310–1315.
[34]A.C. Onicha, N. Petchsang, T.H. Kosel, M. Kuno, ACS Nano 6 (2012) 2833–2843.
[35]M. Afzaal, D.J. Crouch, P. O'Brien, J. Raftery, P.J. Skabara, A.J. White, D.J. Williams, J. Mater. Chem. 14 (2004) 233–237.
[36]M. Akhtar, M.A. Malik, J. Raftery, P. O'Brien, J. Mater. Chem. A 2 (2014) 20612– 20620.
[37]N. Levesanos, W.P. Liyanage, E. Ferentinos, G. Raptopoulos, P. Paraskevopoulou, Y. Sanakis, A. Choudhury, P. Stavropoulos, M. Nath, P. Kyritsis, Eur. J. Inorg. Chem. 2016 (2016) 5332–5339.
[38]P. Musetha, N. Revaprasadu, G. Kolawole, R.V. Pullabhotla, K. Ramasamy, P. O'Brien, Thin Solid Films 519 (2010) 197–202
[39]S. Mahboob, S.N. Malik, N. Haider, C. Nguyen, M.A. Malik, P. O'Brien, J. Cryst. Growth 394 (2014) 39–48.
[40]J. Akhtar, M. Afzaal, M.A. Vincent, N.A. Burton, J. Raftery, I.H. Hillier, P. O'Brien, J. Phys. Chem. C 115 (2011) 16904–16909.
[41]P. Kevin, S.N. Malik, M.A. Malik, P. O'Brien, Chem. Commun. 50 (2014) 14328– 14330.
[42]A. Singhal, D. Dutta, S. Kulshreshtha, S. Mobin, P. Mathur, J. Organomet. Chem. 691 (2006) 4320–4328.
[43]C.Q. Nguyen, M. Afzaal, M.A. Malik, M. Helliwell, J. Raftery, P. O'Brien, J. Organomet. Chem. 692 (2007) 2669–2677.
[44]Y.-J. Hsu, C.-M. Hung, Y.-F. Lin, B.-J. Liaw, T.S. Lobana, S.-Y. Lu, C. Liu, Chem. Mater. 18 (2006) 3323–3329
[45]W. Maneeprakorn, C.Q. Nguyen, M.A. Malik, P. O'Brien, J. Raftery, Dalton Trans. (2009) 2103–2108.
[46] Gong, F.; Wang, H.; Xu, X.; Zhou, G.; Wang, Z.-S. J. Am. Chem. Soc. 2012, 134, 10953−10958.
[47] Jia, J.; Wu, J.; Tu, Y.; Huo, J.; Zheng, M.; Lin, J.. J. Alloys Compd. 2015, 640, 29−33.
[48] Duan, Y.; Tang, Q.; Liu, J.; He, B.; Yu, L. Angew. Chem., Int. Ed. 2014, 53, 14569−14574.
[49] Liu, J.; Tang, Q.; He, B.; Yu, L.. J. Power Sources 2015, 282, 79−86.
[50] Duan, Y.; Tang, Q.; He, B.; Li, R.; Yu, L.. Nanoscale 2014, 6, 12601−12608.
[51] Z.P. Li, H.T. Xue, J.Q. Wang, Y.B. Tang, C.S. Lee, S.R. Yang. Chem Electro Chem. 2 (2015) 1682-1686.
[52]A.H. Thompson, J.C. Scanlon, C.R. Symon, Solid State Ionics 1 (1980) 47-57.
[53] D.M. Pasquariello, K.M. Abraham, Mat. Res. Bull. 22 (1987) 37-44.
[54]J. Morales, J. Santos, J.L. Tirado, Solid State Ionics. 83 (1996) 57-64.
[55] L.W. Mi, H. Sun, Q. Ding, W.H. Chen, C.T. Liu, H.W. Hou, Z. Zheng, C.Y. Shen, Dalton Trans. 41 (2012) 12595
[56]M.Z. Xue, Z.W. Fu, Electrochem. Commun. 8 (2006) 1855-1862.
[57]L.W. Mi, H. Sun, Q. Ding, W.H. Chen, C.T. Liu, H.W. Hou, Z. Zheng, C.Y. Shen, Dalton Trans. 41 (2012) 12595
[58] M.Z. Xue, Y.N. Zhou, B. Zhang, L. Yu, H. Zhang, Z.W. Fu, J. Electrochem. Soc, 153 (2006) A2262-A2268.
[59] H. Okimura, T. Matsumae, Thin Solid Films, 71 (1980) 53-59.
[60]D.J. Crouch, P.M. Hatton, M. Helliwell, P. O'Brien, J. Raftery, Dalton Trans. (2003) 2761 2766.
[61]A. Banerjee, S. Bhatnagar, K.K. Upadhyay, P. Yadav, S. Ogale, ACS Appl. Mater. Interfaces. 6 (2014) 18844-18852.
[62] N. Yu, M.Q. Zhu, D. Chen, J. Mater. Chem. A. 3 (2015) 7910-7918.

IJARSCT
International Journal of Advanced Research in Science, Communication and Technology
International Open-Access, Double-Blind, Peer-Reviewed, Refereed, Multidisciplinary Online Journal
ISSN: 2581-9429 Volume 6, Issue 8, April 2026 Impact Factor: 8.2

[63] W.T. Wei, L.W. Mi, Y. Gao, Z. Zheng, W.H. Chen, X.X. Guan, Chem. Mater. 26 (2014) 3418-3426.
[64] A.H. Loo, A. Bonanni, Z. Sofer, M. Pumera, Electrochem. Commun. 50 (2015) 39-42
[65]C. Tang, N. Cheng, Z. Pu, W. Xing, X. Sun, Angew. Chem. Int. Ed. 54 (2015)
[66] M. Saeed, Y. Alshammari, S. A. Majeed, and E. Al-Nasrallah, "Molecules, vol. 25. (2020) 17. 2020 9351–9355.
[67] J. Lin, H. Wang, Y. Yan, J. Cao, C. Qu, X. Zheng, J. Feng, J. Qi, J. Power Sources (2020).445
[68] F. Jing, Q. Lv, Q. Wang, K. Chi, Z. Xu, X. Wang, S. Wang, Electro. Acta 304 (2019) 202–209.
[69]Y. Chen, Z. Ren, H. Fu, X. Zhang, G. Tian, H. Fu, Small 2018 14.
[70] Y. Zhong, B. Chang, Y. Shao, C. Xu, Y. Wu, X. Hao, ChemSusChem 12 (2019) 2008 2014.
[71] H.-B. Wang, Y.-S. Sun, F. Ma, L. Zhou, H.-F. Li, L. Zhang, G.-J. Chen, Y.-K. Xu, Y.- N. Chen, K.-W. Xu, D.-Y. Ma, J. Alloys Compd. (2020).819
[72] L. Tie, Y. Liu, S. Shen, C. Yu, J. Sun, J. Sun, Appl. Surf. Sci. (2020).526
[73]P. Chen, K. Xu, S. Tao, T. Zhou, Y. Tong, H. Ding, L. Zhang, W. Chu, C. Wu, Y. Xie, Adv. Mater. 28 (2016) 7527–7532.
[74] N. Xue, Z. Lin, P. Li, P. Diao, Q. Zhang, A.C.S. Appl, Mater. Inter. 12 (2020) 28288–28297.
[75] Y.R. Zheng, P. Wu, M.R. Gao, X.L. Zhang, F.Y. Gao, H.X. Ju, R. Wu, Q. Gao, R. You, W.X. Huang, S.J. Liu, S.W. Hu, J. Zhu, Z. Li, S.H. Yu, Nat. Commun. 9 (2018) 2533.
[76] Y. Zhao, B. Jin, Y. Zheng, H. Jin, Y. Jiao, S.-Z. Qiao, Adv. Energy Mater. 8 (2018) 1801926
[77] Fatema Tuz Zohora Toma1*, Md. Sharifur Rahman2, Kazi Md. Amjad Hussain1, Syed Ahmed1- J Mod Nanotechnol, 2024; 4: 6.
[78] Shreya, P. Phogat, R. Jha, and S. Singh, Transit. Met. Chem., vol. 48(2023) 167–183.
[79] Zhitong Jin, Meirong Zhang, Min Wang, Chuanqi Feng, and Zhong-Sheng
[80] Abdul Kareem, Hrudeswar Mohanty, Kathavarayan Thenmozhi, Sudhagar Pitchaimuthu, Sellappan Senthilkumar- ACS Appl. Nano Mater. 2024, 7, 5, 4886–4894